

Peierls transition in the presence of finite-frequency phonons in the one-dimensional extended Peierls-Hubbard model at half-filling

Pinaki Sengupta,¹ Anders W. Sandvik,² and David K. Campbell³

¹*Department of Physics, University of California, Davis, California 95616*

²*Department of Physics, Åbo Akademi University, Porthansgatan 3, FIN-20500, Turku, Finland*

³*Departments of Physics and of Electrical and Computer Engineering, Boston University, 44 Cummington Street, Boston, Massachusetts 02215*

(Dated: June 14, 2018)

We report quantum Monte Carlo (stochastic series expansion) results for the transition from a Mott insulator to a dimerized Peierls insulating state in a half-filled, 1D extended Hubbard model coupled to optical bond phonons. Using electron-electron (e-e) interaction parameters corresponding approximately to polyacetylene, we show that the Mott-Peierls transition occurs at a finite value of the electron-phonon (e-ph) coupling. We discuss several different criteria for detecting the transition and show that they give consistent results. We calculate the critical e-ph coupling as a function of the bare phonon frequency and also investigate the sensitivity of the critical coupling to the strength of the e-e interaction. In the limit of strong e-e couplings, we map the model to a spin-Peierls chain and compare the phase boundary with previous results for the spin-Peierls transition. We point out effects of a nonlinear spin-phonon coupling neglected in the mapping to the spin-Peierls model.

PACS numbers: 75.40.Gb, 75.40.Mg, 75.10.Jm, 75.30.Ds

I. INTRODUCTION

Almost half a century ago, Peierls demonstrated that a one-dimensional (1D) metal coupled to an elastic lattice could exhibit an instability towards a lattice distortion of wave vector $q = 2k_F$.¹ This leads to a gap in the electronic spectrum at the Fermi energy and, for the case of a half-filled band, the ground state is dimerized. Experimentally, the Peierls instability can be observed in a wide range of quasi-1D materials, e.g., conjugated polymers,² organic charge transfer salts,³ MX salts,⁴ and CuGeO_3 .⁵ To explain quantitatively the properties of these materials, several different models extending beyond the original non-interacting Peierls model with a classical lattice have been proposed.⁶ These include the Su-Schrieffer-Heeger (SSH) model,^{7,8,9,10,11} the Holstein model,^{12,13,14} various Peierls-Hubbard^{15,16,17} and extended Peierls-Hubbard^{16,18,19,20,21} models, as well as spin-Peierls models.^{22,23,24,25,26,27,28,29,30,31,32}

The Peierls instability is well understood in the static lattice limit (adiabatic phonons) in the absence of electron-electron (e-e) interactions. The ground state is a Peierls state for arbitrarily small electron-phonon (e-ph) coupling. However, the quantum lattice and e-e interaction effects are still not completely understood. For many quasi-1D materials the zero-point fluctuations of the phonon field are comparable to the amplitude of the Peierls distortion,⁹ and this has spurred a large number of studies of quantum fluctuations in SSH,^{8,10,11} and Holstein,^{13,14} models. Recent numerical studies have shown that quantum fluctuations destroy the Peierls instability for small e-ph coupling and/or large phonon frequency in both the spinless²⁵ and spin- $\frac{1}{2}$ Holstein models¹⁴ at half-filling. For the SSH model, Fradkin and Hirsch¹⁰ carried out an extensive study of spin- $\frac{1}{2}$ ($n = 2$) and spinless ($n = 1$) fermions. In the anti-

adiabatic limit (vanishing ionic mass), they mapped the system to an n -component Gross-Neveu model, which is known to have long-ranged dimerization for arbitrary coupling for $n \geq 2$ but not for $n = 1$. For non-zero ionic mass, a renormalization group analysis showed that the low-energy behavior of the $n = 2$ model is still governed by the zero mass limit of the theory. This implies that the spin- $\frac{1}{2}$ SSH model (but not the spinless model) has a dimerized ground state for arbitrarily weak e-ph coupling. Early numerical calculations are also consistent with this scenario.¹⁰ It should be noted, however, that a dimerized state was also predicted for any non-zero e-ph coupling in the spin- $\frac{1}{2}$ Holstein model,¹³ for which more recent large-scale calculations have instead indicated a non-zero critical coupling.¹⁴

Independent-electron models, such as SSH and Holstein, are important from a theoretical standpoint but are not sufficient to account quantitatively for the experimentally observed properties of real materials. For that e-e interactions have to be included in addition to the e-ph couplings.² The interplay among the different interactions gives rise to a rich variety of broken-symmetry ground states as well as low-energy electron-lattice excitations like solitons, polarons, bipolarons, etc.² At half-filling, on-site (Hubbard) interactions open a charge gap,³³ and in the absence of e-ph couplings the system is then a Mott insulator with algebraically decaying ($1/r$ as a function of distance r) spin-spin correlations. Hence, the Peierls transition in this case is accompanied only by the opening of a spin gap, the charge gap already generated by the e-e interactions. Longer-range e-e interactions can destroy the Mott state, however, and hence must affect also the Mott-Peierls transition. Without phonons, even in the simplest half-filled extended Hubbard model with only on-site (U) and nearest-neighbor (V) interactions,^{34,35} some features of the phase diagram

are still controversial.^{36,37,38,39} Adding e-ph interactions further increases the complexity of the problem, and the determination of the phase diagram remains a very challenging problem.

Zimanyi et al.¹⁹ have investigated models with both e-e and e-ph interactions using “g-ology” and RG techniques. They showed that the ground state has a spin gap if the combined backscattering amplitude $g_1^T = g_1(\omega_0) + \tilde{g}_1(\omega_0)$ is negative, where $g_1(\omega_0)$ is the contribution from e-e interactions and $\tilde{g}_1(\omega_0) < 0$ comes from the e-ph interactions. Thus, in the extended Hubbard model, if the bare coupling $g_1 = U - 2V$ is positive, then $g_1^T \geq 0$ for small values of the e-ph coupling and there is no spin gap. The transition to a Peierls state occurs only when the e-ph coupling exceeds a critical value and g_1^T becomes negative. It should be noted, however, that the conventional scenario for the behavior close to the line $U = 2V$ has recently been challenged^{36,37,39} and a Peierls-like bond-ordered state most likely appears close to $V = U/2$ *even in the absence of e-ph couplings*. For the pure SSH model ($U = V = 0$), g_1 is zero and g_1^T is negative for any non-zero e-ph coupling. This implies a Peierls ground state for arbitrarily small e-ph coupling, in agreement with the earlier results of Fradkin and Hirsch.¹⁰

In the limit of strong on-site e-e interactions, which inhibit doubly occupied sites, a half-filled system can be mapped to a spin-phonon model, which also can undergo a dimerization (spin-Peierls) transition.^{22,24} Extensive studies of spin-Peierls models in recent years^{26,27,28,29,30,31,32} have largely been spurred by the discovery of a spin-Peierls transition at unusually high temperature (14 K) in CuGeO_3 .⁵ Several different calculations, for different types of spin-phonon couplings, have shown that the transition occurs only above a finite spin-phonon coupling in the presence of finite-frequency phonons.^{26,29,30,31,32} This is in contrast to the adiabatic limit, where dimerization occurs for infinitesimal coupling.²⁴

Numerical studies of models with both e-ph and e-e interactions, in which the charge degrees of freedom are retained (Peierls-Hubbard and extended Peierls Hubbard models), have addressed the effect of interactions on the dimerization amplitude^{16,18} and the excited states.²¹ Detailed studies of the phase diagrams have in the past been limited by the small lattice sizes accessible when both e-e and e-ph interactions are included.¹⁷ The situation is rapidly improving, however, as modern quantum Monte Carlo^{29,37,40} and density matrix renormalization group^{21,30} methods can now access models with both e-e and e-ph interactions on chains with several hundred sites.

Here we consider a 1D extended Hubbard model with on-site (U) and nearest-neighbor (V) e-e interactions and couple it to dispersionless optical bond phonons via modulation of the electron kinetic energy. We study the transition from a Mott insulating state, with dominant spin-spin correlations, to a Peierls (dimerized) spin-gapped state. Since the parameter space of this model is rather

large, with a bare phonon frequency (ω_0) and an e-ph coupling (α) in addition to the e-e couplings, we have limited our study to a physically reasonable ratio $U/V = 4$ of the e-e parameters.

In Sec. II we define the model and the various physical quantities that we have calculated using a quantum Monte Carlo method (stochastic series expansion⁴⁰). In Sec. III we discuss several signals that we have used to detect the Mott-Peierls transition. In Sec. IV we present the phase diagram in the (ω_0, α) -plane for a fixed value of the on-site interaction U that has previously been used in models of polyacetylene. We also discuss the effects of varying the e-e interaction strength at fixed ω_0 . We map the model to a spin-Peierls model for large U, V and compare the Mott-Peierls boundary with known spin-Peierls results. In Sec. V we summarize our results and discuss some future prospects.

II. MODEL AND OBSERVABLES

The Hamiltonian is given by

$$\begin{aligned}
 H = & -t \sum_{i,\sigma} (1 + \alpha[a_i^\dagger + a_i]) (c_{i+1,\sigma}^\dagger c_{i,\sigma} + c_{i,\sigma}^\dagger c_{i+1,\sigma}) \\
 & + \mu \sum_i n_i + U \sum_i (n_{i,\uparrow} - \frac{1}{2})(n_{i,\downarrow} - \frac{1}{2}) \\
 & + V \sum_i (n_i - 1)(n_{i+1} - 1) + \omega_0 \sum_i a_i^\dagger a_i, \quad (1)
 \end{aligned}$$

where $a_i^\dagger(a_i)$ creates(annihilates) a phonon on the bond between sites i and $i + 1$, $c_{i,\sigma}^\dagger(c_{i,\sigma})$ is the spin- σ electron creation(annihilation) operator, and $n_i = n_{i,\downarrow} + n_{i,\uparrow}$. For the half-filled band that we study here, the chemical potential $\mu = 0$. We set the single-electron hopping t to unity. For the e-e interactions, we first take the values $U = 2.5$, $V = U/4$, which have previously been used as values corresponding approximately to what is expected in polyacetylene.²⁰ We will also consider other values of U , keeping the ratio fixed at $U/V = 4$. We study the system as a function of the bare phonon frequency ω_0 and the e-ph interaction α .

The dispersionless optical phonons we use are different from the bare SSH phonons, which have vanishing energy for momentum $q \rightarrow 0$. However, these acoustic phonons decouple from the electronic low-energy states involved in the Peierls instability and therefore only the optical phonons close to $q = \pi$ need to be kept.^{10,19} Hence, in this regard we expect the optical phonons in (1) to be equivalent to fully quantum mechanical SSH phonons. In the non-interacting limit ($U, V \rightarrow 0$), the ground state should therefore be a dimerized Peierls insulator for any non-zero α .¹⁰

To obtain numerically exact ground state results we have used the stochastic series expansion (SSE) quantum Monte Carlo method⁴⁰ for periodic chains with up to $N = 256$ sites. The SSE method is a finite-temperature

technique based on importance sampling of the diagonal elements of the Taylor expansion of $e^{-\beta H}$, where β is the inverse temperature; $\beta = t/T$. Ground state expectation values can be obtained using sufficiently large β , and there are then no approximations beyond the statistical errors. Typically, $\beta = 2N$ or $4N$ was sufficient for the quantities presented here to have converged to their ground state values. Using the recently developed “operator loop” update,⁴⁰ the electronic degrees of freedom are treated in the same manner as in the absence of phonons.³⁷ The phonons are also treated in the occupation number basis directly with the SSE representation⁴¹ (i.e., slightly different from the interaction picture used for the phonons in in Refs. 29 and 42). At the (low) energy scales that we are interested in here, the number of phonons per bond is small (typically < 10) and there are no problems in using a truncated basis (the truncation can be arbitrarily large in the SSE).

The Mott and Peierls phases can be characterized using the static spin (S) and bond (B) structure factors and susceptibilities, as will be further discussed in Sec. III. The structure factors are defined by

$$S_S(q) = \frac{1}{N} \sum_{k,l} e^{iq(k-l)} \langle S_k^z S_l^z \rangle, \quad (2)$$

$$S_B(q) = \frac{1}{N} \sum_{k,l} e^{iq(k-l)} \langle K_k K_l \rangle, \quad (3)$$

where $K_j = \sum_{\sigma=\uparrow,\downarrow} (c_{j+1,\sigma}^\dagger c_{j,\sigma} + \text{h.c.})$ is the kinetic energy operator on the i th bond. The corresponding static susceptibilities are given by

$$\chi_S(q) = \frac{1}{N} \sum_{k,l} e^{iq(k-l)} \int_0^\beta d\tau \langle S_k^z(\tau) S_l^z(0) \rangle, \quad (4)$$

$$\chi_B(q) = \frac{1}{N} \sum_{k,l} e^{iq(k-l)} \int_0^\beta d\tau \langle K_k(\tau) K_l(0) \rangle. \quad (5)$$

Direct evidence for the presence or absence of the spin and charge gaps can also be obtained from spin and charge stiffnesses ρ_c and ρ_s , which are defined as the second derivative of the internal energy per site with respect to phase factors multiplying the kinetic energy; $\rho_{c,s} = \partial^2 E(\phi_{c,s}) / \partial \phi_{c,s}^2$.⁴³ The SSE estimators for all these observables can be found in Ref. 37.

III. DETECTING THE MOTT-PEIERLS TRANSITION

For our choice of $V = U/4$, the ground state in the limit of zero e-ph interaction ($\alpha = 0$) is a Mott insulator with no spin gap (but finite charge gap) and is characterized by a $1/r$ decay of the staggered spin-spin correlations.^{35,37} The transition to a dimerized Peierls state is marked by the development of a staggered kinetic energy modulation and will hence be signalled by divergent peaks at

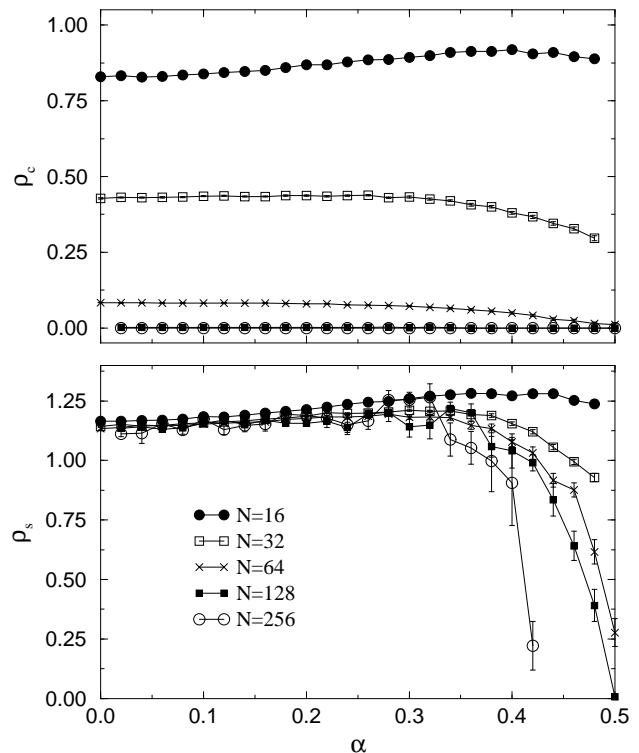


FIG. 1: Charge (upper panel) and spin (lower panel) stiffness constants vs e-ph coupling for several different system sizes at $\omega_0 = 1$ and $U = 2.5$.

$q = \pi$ in the bond-order structure factor, Eq. (3), and susceptibility, Eq. (5). The dimerization is accompanied by the opening of a spin gap, the charge gap remaining finite. Hence the $q = \pi$ peak in the spin structure factor and susceptibility, Eqs. (2) and (4), which diverge in the Mott phase, become non-divergent in the Peierls state.

In the adiabatic limit, the system is dimerized for any $\alpha > 0$. We here present several results showing that the Peierls transition occurs at a critical coupling $\alpha_c > 0$ when $\omega_0 = 1$ and $U = 2.5$. The phase diagrams discussed in Sec. IV are based on the same signals for the transition at other e-e couplings and ω_0 .

Since the charge gap is finite in both the Mott and Peierls states, the charge stiffness ρ_c should vanish in the thermodynamic limit for all α . The upper panel of Fig. 1 shows ρ_c as a function of α for several system sizes N . As N grows, ρ_c indeed rapidly converges to zero for all α , in agreement to our expectations. The Mott state has no spin gap (finite spin stiffness) whereas the Peierls state has a finite spin gap (zero spin stiffness). If the Peierls transition occurs at a critical coupling $\alpha_c > 0$, it should be of the Kosterlitz-Thouless type,³⁵ where the spin stiffness changes discontinuously from a finite value for $\alpha \leq \alpha_c$ to zero for $\alpha > \alpha_c$. The spin stiffness graphed in the lower panel of Fig. 1 shows a jump developing with increasing N , indicating a critical coupling $\alpha_c \approx 0.3$.

The spin stiffness data do not easily yield a more accurate estimate of the critical coupling. As discussed in

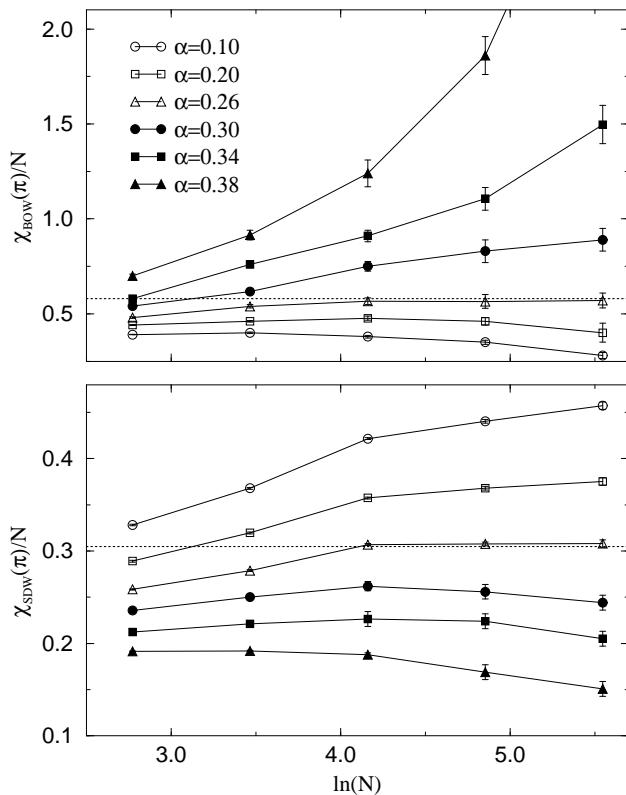


FIG. 2: Finite-size scaling of the staggered bond-order (upper panel) and spin (lower panel) susceptibility for $\omega_0/t = 1$ and several values of α . The dashed lines show the N -independent behavior expected at the Mott-Peierls transition.

the context of the spin-Peierls model,²⁹ logarithmic corrections lead to large finite-size effects for $\alpha \approx \alpha_c$. A more accurate estimate can be obtained from the scaling behavior of the finite-size staggered bond and spin susceptibilities.²⁹ It is known from bosonization studies that in the Mott phase the equal-time staggered spin and bond correlations both decay with distance r as $1/r$, up to multiplicative logarithmic corrections.³⁵ At the Mott-Peierls phase boundary, the log-corrections can be expected to disappear,⁴⁴ and this can be used as a criterion for the phase transition. In the dimerized Peierls phase the bond correlation function approaches a constant at long distances, whereas the spin correlations decay exponentially. It is convenient to study the associated static susceptibilities defined in Eqs. (4) and (5), which in a critical state scale with one power of N higher than the structure factors Eqs. (2) and (3). In the Peierls phase $\chi_S(\pi)/N$ should converge to 0 and $\chi_B(\pi)/N$ should diverge, whereas in the Mott phase $\chi_S(\pi)/N$ should diverge logarithmically and $\chi_B(\pi)/N$ should approach zero logarithmically (the log-corrections for spin and bond correlations are different³⁵). Fig. 2 shows both quantities versus $\ln(N)$ for several values of α . The expected behavior is indeed observed, and within statistical errors both $\chi_S(\pi)/N$ and $\chi_B(\pi)/N$ are independent of N for

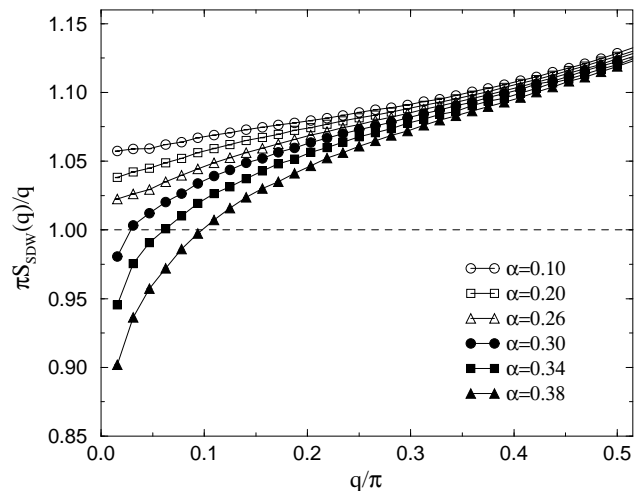


FIG. 3: $S_S(q)/q$ vs q for several values of α around α_c for $N=128$. The curves for $\alpha \geq 0.30$ dip below 1 for small q , indicating the presence of a spin-gap.

the largest chains when $\alpha \approx 0.26$.

Additional confirmation of the critical coupling is obtained by studying the behavior of $S_S(q)/q$ as $q \rightarrow 0$. It has been shown^{35,45} that if the ground state is gapless in the spin sector, then $S_S(q)/q \rightarrow 1/\pi$ as $q \rightarrow 0$, whereas if there is a spin gap, $S_S(q)/q \rightarrow 0$. Even a very small spin gap can be detected this way, since it is in practice sufficient to see that $\pi S_S(q)/q$ decays below 1 for small q to conclude that a spin gap must be present. In Fig. 3 we present results for different values of α . The curves for $\alpha \leq 0.26$ are above 1 for all q , and the decay towards 1 is very slow. The asymptotic approach to 1 can be expected to be logarithmic.⁴⁶ On the other hand, the $\alpha \geq 0.30$ curves drop below 1. From these results we estimate $\alpha_c = 0.28 \pm 0.01$, which is compatible with the $q = \pi$ quantities in Fig. 2. In general, we have found that $S_S(q)/q$, which indirectly signals the opening of a spin gap, is the easiest and most reliable way to detect a bond-ordered state (see also Ref. 37).

IV. PHASE DIAGRAMS

The critical coupling depends on the parameters of the Hamiltonian, in particular, the bare phonon frequency ω_0 . Using the above criteria for distinguishing the Mott and Peierls phases, we have calculated α_c as a function of ω_0 , keeping $U = 2.5$, $V = 0.625$. As shown in Fig. 4, α_c decreases linearly to zero for small ω_0 . This phase diagram is hence consistent with the known $\alpha_c = 0$ for adiabatic phonons.

For polyacetylene Fradkin and Hirsch¹⁰ used rescaled phonon parameters, which in our units correspond to $\omega_0 = 0.067$, $\alpha = 0.052$. This point is indicated in Fig. 4, and, in accordance with the strong dimerization of polyacetylene, is well within the Peierls phase.

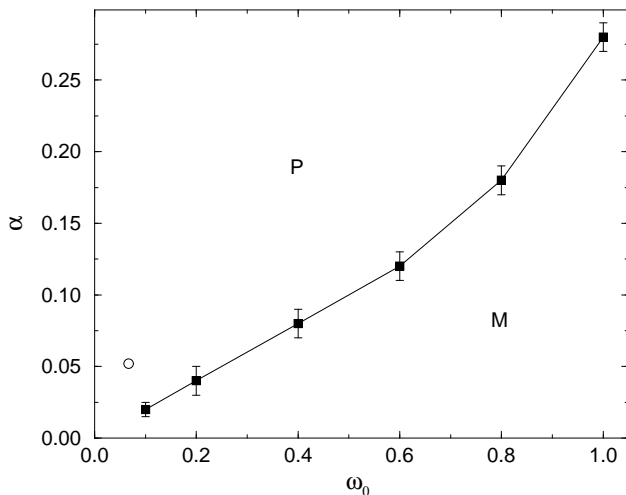


FIG. 4: Phase diagram for $U=2.5$, $V=0.625$. The squares with error bars show the critical e-ph coupling separating the Mott (M) and Peierls (P) insulating phases. The circle corresponds to phonon parameters previously used for polyacetylene.¹⁰

As argued above, the e-ph coupling in the present model is similar to that in the SSH model for the purpose of studying the dimerization transition. This implies that in the limit of $(U, V) \rightarrow 0$, we should be able to reproduce previous SSH results. In particular, according to Fradkin and Hirsch,¹⁰ α_c should be zero even for finite frequency phonons. To verify this, we have studied α_c as a function of (U, V) , keeping a fixed ratio of $U/V = 4$. With this ratio the ground state for all U is a Mott insulator with zero spin gap in the limit of vanishing e-ph interaction.³⁷ We have studied only a single phonon frequency, $\omega_0 = 1$. The resulting phase diagram is presented in Fig. 5. The critical e-ph coupling decreases monotonically with decreasing (U, V) , but the smallness of the spin gap as $(U, V) \rightarrow 0$ makes it hard to obtain reliable results below $U = 0.4$. We can therefore not make a definite statement about this limit. Nevertheless, our results are consistent with a power-law behavior $\alpha_c \sim U^\gamma$ with $\gamma \approx 0.3$, but a logarithmic form for $U \rightarrow 0$ can also not be excluded.

For large U, V , and with the ratio $V = U/4$, the extended Hubbard model can be mapped onto the spin- $\frac{1}{2}$ Heisenberg chain with exchange coupling $J = 4t^2/(U - V)$ (this mapping becomes invalid for $V \approx U/2$, where phase transitions to bond-ordered and charge-ordered phases occur^{35,36,37}). Carrying out this transformation for the full electron-phonon model (1), the phonon-modulated exchange is

$$J(x_i) = \frac{4t^2(1 + \alpha x_i)^2}{U - V}, \quad (6)$$

where $x_i = a_i^\dagger + a_i$. Under the assumption that the nonlinear term $\sim (\alpha x_i^2)$ can be neglected, which is not *a priori* clear when α is not small, we obtain exactly the

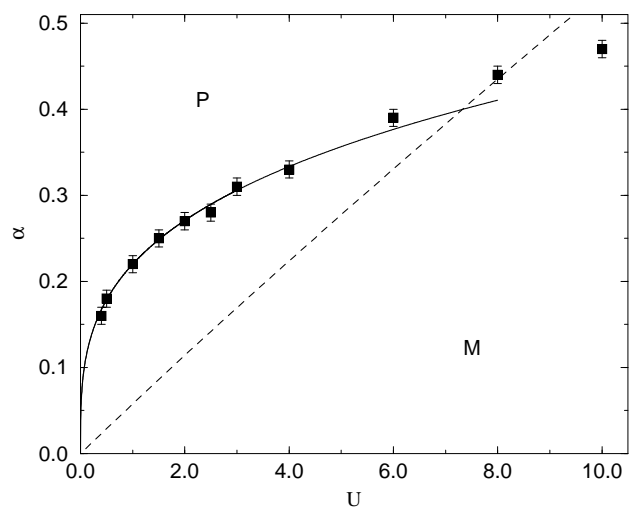


FIG. 5: Phase diagram for $\omega_0 = 1, V = U/4$. The squares with error bars show the critical e-ph coupling. The solid curve shows the form $\alpha_c \sim U^{0.3}$. The dashed curve shows the transition for the corresponding spin-Peierls model.³²

spin-Peierls model considered in, e.g., Refs. 29 and 32:

$$H_{\text{SP}} = \sum_i (J + gx_i) \mathbf{S}_i \cdot \mathbf{S}_{i+1} + \omega_0 \sum_i a_i^\dagger a_i, \quad (7)$$

with

$$J = \frac{4t^2}{U - V}, \quad g = \frac{8\alpha t^2}{U - V}. \quad (8)$$

For the model (7), an analytic expression for the critical spin-phonon coupling g has been obtained for the whole range of bare phonon frequencies ω_0/J .³² The form, Eq. (12) of Ref. 32, is expected to be exact in the anti-adiabatic limit, $\omega_0/J \rightarrow \infty$, which here corresponds to $U \rightarrow \infty$. It is in good agreement with numerical (SSE) results²⁹ for the spin-Peierls transition even for frequencies as low as $\omega_0/J = 0.25$. In Fig. 5 we compare our SSE results for the extended Peierls-Hubbard model with the spin-Peierls form for U up to 10. The transition curve crosses the Mott-Peierls transition curve at $U \approx 8$, and is not in good agreement away from this point. The spin-Peierls critical α increases linearly with U as $U \rightarrow \infty$, whereas the Mott-Peierls boundary has a slower increase with U . The poor agreement for small U is not surprising, as the mapping to the spin chain, with coupling J given by (8), can only be expected to be good for large U , and the form used for the spin-Peierls transition curve is not expected to be quantitatively accurate for very small ω/J (corresponding here to small U).³² Considering, however, that the analytical form is accurate for the spin-Peierls model with $\omega_0/J = 0.25$,^{29,32} and that the nonlinear spin-phonon coupling should be negligible for small α , the disagreement for the small- U region in Fig. 5 must be due to the poor correspondence between the full electron model and the spin chain with

the lowest-order J in Eq. (8). The poor agreement for $U > 8$ indicates that the nonlinear spin-Phonon term $(\alpha x_i)^2$ does becomes important as $U \rightarrow \infty$.

One effect of the nonlinear coupling term is to renormalize J : Writing $x_i^2 = \langle x_i^2 \rangle + \Delta(x_i^2)$, the renormalized J is given by

$$J_{\text{eff}} = \frac{4t^2(1 + \alpha^2 \langle x_i^2 \rangle)}{U - V}, \quad (9)$$

i.e., $J_{\text{eff}} > J$. Evaluation the spin-Peierls transition curve using J_{eff} instead of J clearly would reduce α_c for given U and bring the result closer to the actual Mott-Peierls curve in Fig. 5. However, we have not evaluated $\langle x_i^2 \rangle$ for a quantitative test of this effect. In any case, if $\langle x_i^2 \rangle$ is large there is also no reason to expect that the remaining nonlinear coupling $\Delta(x_i^2)$ can be neglected if α is not small. This issue clearly deserves further study.

V. SUMMARY

In summary, we have studied several aspects of the phase diagram of an extended 1D Hubbard model coupled to optical bond phonons. We have demonstrated that the stochastic series expansion technique^{37,40} can be used for large electron-phonon chains (here up to 256 sites) to compute several different quantities that signal the opening of the spin gap at the Mott-Peierls transition. The spin gap boundary is also in good agreement with direct probes of the bond order (i.e., kinetic-energy correlation functions and susceptibilities at $q = \pi$).

Our phase diagrams are in agreement with what is generally expected, but to our knowledge they have not been computed quantitatively before. For large e-e couplings, we have pointed out the relevance of an effective nonlinear spin-phonon coupling in the mapping of the Hubbard model to a spin chain. Because of this, standard spin-phonon models, where the nonlinear term is not included, cannot be expected to reproduce fully the phase diagrams of electron-phonon models.

The methods that we have used here should also be applicable to systems away from half-filling. We plan such calculations aimed at studying the stability of the soliton lattice, which is formed in doped systems in the adiabatic limit,^{7,20,47} in the presence of finite-frequency phonons. A previous quantum Monte Carlo study has indicated that the soliton lattice is stable.¹⁶ However, open boundary conditions were used for relatively small chains, and therefore the issue of whether this is a stable phase on an infinite lattice remains to be clarified.

Acknowledgments

This work was supported by the NSF under Grants No. DMR-99-86948 (PS) and DMR-97-12765 (DKC), and by the Academy of Finland, project 26175 (AWS). The numerical calculations were carried out at the NCSA in Urbana, Illinois.

¹ R. E. Peierls, *Quantum Theory of Solids*, (Oxford, 1955).

² H. G. Keiss (ed.), *Conjugated Conducting Polymers*, (Springer-Verlag, Berlin, 1992).

³ T. Ishiguro and K. Yamaji, *Organic Superconductors*, (Springer-Verlag, Berlin, 1990).

⁴ H. Toftlund and O. Simonsen, *Inorg. Chem.* **23**, 4261 (1984).

⁵ M. Hase, I. Terasaki and K. Uchinokura, *Phys. Rev. Lett.* **70**, 3651 (1993).

⁶ For a review, see D. Baeriswyl, D. K. Campbell, and S. Mazumdar, in Ref. 2.

⁷ W. P. Su, J. R. Schrieffer and A. J. Heeger, *Phys. Rev. Lett.* **42**, 1698 (1979); *Phys. Rev. B* **22**, 2099 (1980); **28**, 1138E (1983).

⁸ M. Nakahara and K. Maki, *Phys. Rev. B* **25**, 7789 (1982).

⁹ W. P. Su, *Solid State Commun.* **42**, 497 (1982).

¹⁰ E. Fradkin and J. E. Hirsch, *Phys. Rev. B* **27**, 1680 (1983).

¹¹ H. Zheng, *Phys. Rev. B* **50**, 6717 (1994).

¹² T. Holstein, *Ann. Phys.* **8**, 325 (1959); **8**, 343 (1959).

¹³ J. E. Hirsch and E. Fradkin, *Phys. Rev. B* **27**, 4302 (1983).

¹⁴ E. Jeckelmann, C. Zhang and S. R. White, *Phys. Rev. B* **60**, 7950 (1999).

¹⁵ D. Baeriswyl, J. P. Carmelo, and K. Maki, *Synth. Met.* **21**, 271 (1987); E. Jeckelmann, and D. Baeriswyl, *ibid.* **65**, 211

(1994); G. Wen and W.-P. Su, *ibid.* **78**, 195 (1996).

¹⁶ A. Takahashi, *Phys. Rev. B* **54**, 7965 (1996).

¹⁷ H. Fehske, A. P. Kampf, M. Sekania, and G. Wellein, *cond-mat/0203616*.

¹⁸ J. E. Hirsch, *Phys. Rev. B* **31**, 6022 (1985).

¹⁹ G. T. Zimanyi, S. A. Kivelson and A. Luther, *Phys. Rev. Lett.* **60**, 2089 (1988); G. T. Zimanyi and S. A. Kivelson, *Mol. Cryst. Liq. Cryst.* **160**, 457 (1988).

²⁰ E. Jeckelmann, *Phys. Rev. B* **57**, 11 838 (1998).

²¹ W. Barford, R. J. Bursill, and M. Y. Lavrentiev, *Phys. Rev. B* **65** 075107 (2002)

²² P. Pincus, *Solid State Comm.* **9**, 1971 (1971).

²³ E. Pytte, *Phys. Rev. B* **10**, 4637 (1974).

²⁴ M. C. Cross and D. S. Fisher, *Phys. Rev. B* **19**, 402 (1979).

²⁵ R. J. Bursill, R. H. McKenzie and C. J. Hamer, *Phys. Rev. Lett.* **80**, 5607 (1998).

²⁶ G. S. Uhrig, *Phys. Rev. B* **57**, R14004 (1998).

²⁷ C. Gros and R. Werner, *Phys. Rev. B* **58**, R14677 (1998).

²⁸ G. Wellein, H. Fehske, and A. P. Kampf, *Phys. Rev. Lett.* **81**, 3956 (1998).

²⁹ A. W. Sandvik and D. K. Campbell, *Phys. Rev. Lett.* **83**, 195 (1999).

³⁰ R. J. Bursill, R. H. McKenzie and C. J. Hamer, *Phys. Rev. Lett.* **83**, 408 (1999).

³¹ A. Weiße, G. Wellein, and H. Fehske, *Phys. Rev. B* **60**,

- 6566 (1999).
- ³² C. Raas, U. Löw, G. S. Uhrig, and R. W. Kühne, Phys. Rev. B **65**, 144438 (2002).
- ³³ E. H. Lieb and F. Y. Wu, Phys. Rev. Lett. **20**, 1445 (1968).
- ³⁴ J. Sólyom, Advances in Physics, **28**, 201 (1979).
- ³⁵ J. Voit, Phys. Rev. B **45**, 4027 (1992).
- ³⁶ M. Nakamura, J.Phys. Soc. Jpn. **68**, 3123 (1999): Phys. Rev. B **61**, 16377 (2000).
- ³⁷ P. Sengupta, A. W. Sandvik and D. K. Campbell, Phys. Rev. B **65**, 155113 (2002).
- ³⁸ E. Jeckelmann, Phys. Rev. Lett. **89**, 236401 (2002).
- ³⁹ A. W. Sandvik, P. Sengupta, and D. K. Campbell, cond-mat/0301237.
- ⁴⁰ A. W. Sandvik, Phys. Rev. B **59**, 14157 (1999).
- ⁴¹ P. Sengupta, Ph.D. thesis, University of Illinois at Urbana-Champaign, (2001, unpublished).
- ⁴² A. W. Sandvik, R. R. P. Singh, and D. K. Campbell, Phys. Rev. B **56**, 14510 (1997).
- ⁴³ W. Kohn, Phys. Rev. **133**, 171 (1964).
- ⁴⁴ S. Eggert, Phys. Rev. B **54**, R9612 (1996).
- ⁴⁵ R. T. Clay, A. W. Sandvik and D. K. Campbell, Phys. Rev. B **59**, 4665 (1999).
- ⁴⁶ S. Eggert, I. Affleck, and M. Takahashi, Phys. Rev. Lett **73**, 332 (1994).
- ⁴⁷ M. I. Salkola and S. A. Kivelson, Phys. Rev. B **50**, 13962 (1994).